3. Heidenreich R, Natowicz M, Hainline BE, et al. Acute extrapyramidal syndrome in methylmalonic acidemia: "metabolic stroke" involving the globus pallidus. J Pediatr 1988;113:1022–1027.
4. Schwab MA, Sauer SW, Okun JG, et al. Secondary mitochondrial dysfunction in propionic aciduria: a pathogenic role for endogenous mitochondrial toxins. Biochem J 2006;398:107–112.
5. Sauer SW, Opp S, Mahringer A, et al. Glutaric aciduria type I and methylmalonic aciduria: simulation of cerebral import and export of accumulating neurotoxic dicarboxylic acids in in vitro models of the blood-brain barrier and the choroid plexus. Biochim Biophys Acta 2010;1802:552–560.
6. Radmanesh A, Zaman T, Ghanaati H, Molaei S, Robertson RL, Zamani AA. Methylmalonic acidemia: brain imaging findings in 52 children and a review of the literature. Pediatr Radiol 2008;38:1054–1061.
7. Williams ZR, Hurley PE, Altiparmak UE, et al. Late onset optic neuropathy in methylmalonic and propionic acidemia. Am J Ophthalmol 2009;147:929–933.
8. Grunert SC, Mullerleile S, de Silva L, et al. Propionic acidemia: neonatal versus selective metabolic screening. J Inherit Metab Dis 2012;35:41–49.
9. Perez-Cerda C, Merinero B, Rodriguez-Pombo P, et al. Potential relationship between genotype and clinical outcome in propionic acidaemia patients. Eur J Hum Genet 2000;8:187–194.
10. Collins J, Kelly D. Cardiomyopathy in propionic acidemia. Eur J Pediatr 1994;153:53.

Journal of Human Genetics (2013), 1–8

www.nature.com/jhg

ORIGINAL ARTICLE

Exome sequencing identifies a novel *TTN* mutation in a family with hereditary myopathy with early respiratory failure

Rumiko Izumi[1,2], Tetsuya Niihori[1], Yoko Aoki[1], Naoki Suzuki[2], Masaaki Kato[2], Hitoshi Warita[2], Toshiaki Takahashi[3], Maki Tateyama[2], Takeshi Nagashima[4], Ryo Funayama[4], Koji Abe[5], Keiko Nakayama[4], Masashi Aoki[2] and Yoichi Matsubara[1]

Myofibrillar myopathy (MFM) is a group of chronic muscular disorders that show the focal dissolution of myofibrils and accumulation of degradation products. The major genetic basis of MFMs is unknown. In 1993, our group reported a Japanese family with dominantly inherited cytoplasmic body myopathy, which is now included in MFM, characterized by late-onset chronic progressive distal muscle weakness and early respiratory failure. In this study, we performed linkage analysis and exome sequencing on these patients and identified a novel c.90263G>T mutation in the *TTN* gene (NM_001256850). During the course of our study, another groups reported three mutations in *TTN* in patients with hereditary myopathy with early respiratory failure (HMERF, MIM #603689), which is characterized by overlapping pathologic findings with MFMs. Our patients were clinically compatible with HMERF. The mutation identified in this study and the three mutations in patients with HMERF were located on the A-band domain of titin, suggesting a strong relationship between mutations in the A-band domain of titin and HMERF. Mutation screening of *TTN* has been rarely carried out because of its huge size, consisting of 363 exons. It is possible that focused analysis of *TTN* may detect more mutations in patients with MFMs, especially in those with early respiratory failure.
Journal of Human Genetics advance online publication, 28 February 2013; doi:10.1038/jhg.2013.9

Keywords: A-band; cytoplasmic body; Fn3 domain; hereditary myopathy with early respiratory failure; HMERF; myofibrillar myopathy; titin; *TTN*

INTRODUCTION

Myofibrillar myopathies (MFMs) were proposed in 1996 as a group of chronic muscular disorders characterized by common morphologic features observed on muscle histology, which showed the focal dissolution of myofibrils followed by the accumulation of products of the degradative process.[1] The clinical phenotype of MFM is characterized by slowly progressive muscle weakness that can involve proximal or distal muscles, with onset in adulthood in most cases. However, other phenotypes are highly variable. Although 20% of patients with MFMs have been revealed to have mutations in *DES*, *CRYAB*, *MYOT*, *LDB* (*ZASP*), *FLNC* or *BAG3*, the major genetic basis of MFMs remains to be elucidated.

Respiratory weakness is one of the symptoms of MFMs. The early or initial presentation of respiratory failure is not a common manifestation of MFMs as a whole, and there are limited reports regarding a fraction of patients with *DES*,[2] *MYOT*[3] or *CRYAB*[4] mutation. In 1993, our group reported a Japanese family with dominantly inherited cytoplasmic body (CB) myopathy,[5] which is now included in MFM. Currently, this family includes 20 patients in five successive generations who show almost homogeneous clinical features characterized by chronic progressive distal muscle weakness and early respiratory failure. However, the underlying genetic etiology in this family was unknown. The aim of this study was to determine the genetic cause in this family. To identify the responsible genetic mutation, we performed linkage analysis and whole-exome sequencing.

MATERIALS AND METHODS

This study was approved by the Ethics Committee of the Tohoku University School of Medicine, and all individuals gave their informed consent before their inclusion in the study.

[1]Department of Medical Genetics, Tohoku University School of Medicine, Sendai, Japan; [2]Department of Neurology, Tohoku University School of Medicine, Sendai, Japan; [3]Department of Neurology and Division of Clinical Research, National Hospital Organization Nishitaga National Hospital, Sendai, Japan; [4]Division of Cell Proliferation, United Centers for Advanced Research and Translational Medicine, Tohoku University Graduate School of Medicine, Sendai, Japan and [5]Department of Neurology, Okayama University Medical School, Okayama, Japan
Correspondence: Dr Y Aoki, Department of Medical Genetics, Tohoku University School of Medicine, 1-1 Seiryo-machi, Aoba-ku, Sendai 980-8574, Japan.
E-mail: aokiy@med.tohoku.ac.jp
or Professor M Aoki, Department of Neurology, Tohoku University School of Medicine, 1-1 Seiryo-machi, Aoba-ku, Sendai 980-8574, Japan.
E-mail: aokim@med.tohoku.ac.jp
Received 23 October 2012; revised 9 January 2013; accepted 10 January 2013

Clinical information on the family

This family includes 20 patients (13 males and 7 females) in five successive generations (Figure 1). The family is of Japanese ancestry, and no consanguineous or international mating was found. Of all patients, seven underwent a muscle biopsy, and two were autopsied. All of the histological findings were compatible with MFM (see clinical data).

The age of onset ranged from 27–45 years. The most common presenting symptom was foot drop. At the initial evaluations, muscle weakness was primarily distributed in the ankle dorsiflexors and finger extensors. The patients were generally built and showed no other extramuscular abnormalities. In addition to this chronic progressive distal muscle weakness, respiratory distress occurred between 0 and 7 years from the initial onset (average 3.8 years) in seven patients (IV-9, V-2, A, B, E, H, and J) with adequate clinical information. Two patients who had not had any respiratory care died of respiratory failure approximately a decade from the initial onset. The other patients have been alive for more than 10 years (maximum 18 years) but require nocturnal non-invasive positive pressure ventilation. They were 37–58 years of age as of 2012 and able to walk independently with or without a simple walking aid. Although the time at which patients recognized dysphagia or dysarthria varied between 1 to more than 10 years from the initial onset, decreased bulbar functions had been noted at the initial evaluation in most cases. Cardiac function was normally maintained in all patients of the family.

Clinical data

The level of serum creatine kinase was normal or mildly elevated. Electromyography of affected muscles showed a chronic myogenic pattern, and the nerve conduction study did not suggest any neuropathic involvement. Muscle imaging showed focal atrophy in the tibialis anterior, tibialis posterior, extensor hallucis and digitorum longus, peroneal and semitendinosus muscle on initial assessment (Figure 2A), and atrophy became clear in cervical muscles, shoulder girdles, intercostals and proximal limb muscles in the following several years. Upon muscle biopsy, the most common finding was numerous cytoplasmic bodies (CBs), which were found on 7.3% of myofibers in the tibialis anterior of individual E (Figure 2B (a–c)) and 50–80% of intercostals in other cases.[5] Other nonspecific findings were increased variability in the size of myofibers, central nuclei and rimmed vacuoles observed on a few fibers. No strong immunoreaction of desmin was seen in the CBs (Figure 2B (d, e)). An electron microscope examination showed that the regular sarcoplasmic pattern was replaced by abnormal fine filamentous structures, which seemed to attach to the Z-band. CBs were also found in almost all skeletal muscles and some smooth muscles in autopsied cases.[5] Cardiac myofibers also contained numerous CBs in one of the autopsied cases (V-2),[5] although the patient did not present any cardiac complication. The sequence analysis of the coding regions and flanking introns of *DES* and *MYOT* showed no pathogenic mutation in individual E. An array comparative genomic hybridization performed with the Agilent SurePrint G3 Human CGH 1M microarray format in individual A did not reveal any aberrations of genomic copy number.

Linkage analysis

DNA was extracted by standard methods. Linkage analysis was performed on nine family members (A–I in Figure 1; four of them were affected, and the others were unaffected) through genotyping using an Illumina Human Omni 2.5 BeadChip (Illumina, San Diego, CA, USA). We chose single-nucleotide polymorphisms (SNPs) that satisfied all of the following criteria: (1) autosomal SNPs whose allele frequencies were available from the HapMap project (http://hapmap.ncbi.nlm.nih.gov/), (2) SNPs that were not monomorphic among members and (3) SNPs that were not in strong linkage disequilibrium with neighboring SNPs (r2 values <0.9). Then, we selected the first five SNPs from each position of integer genetic distance from SNPs that met the above criteria for the initial analysis. The details were as follows; we chose a SNP closest to 0 cM and the neighboring four SNPs. If the genetic distance of a SNP was the same as that of the next SNP, we considered the genomic position to determine their order. We repeated this process at 1 cM, 2 cM and so on.

We performed a multipoint linkage analysis of the data set (17 613 SNPs) using MERLIN[6] 1.1.2 under the autosomal dominant mode with the following parameters: 0.0001 for disease allele frequency, 1.00 for individuals heterozygous and homozygous for the disease allele and 0.00 for individuals

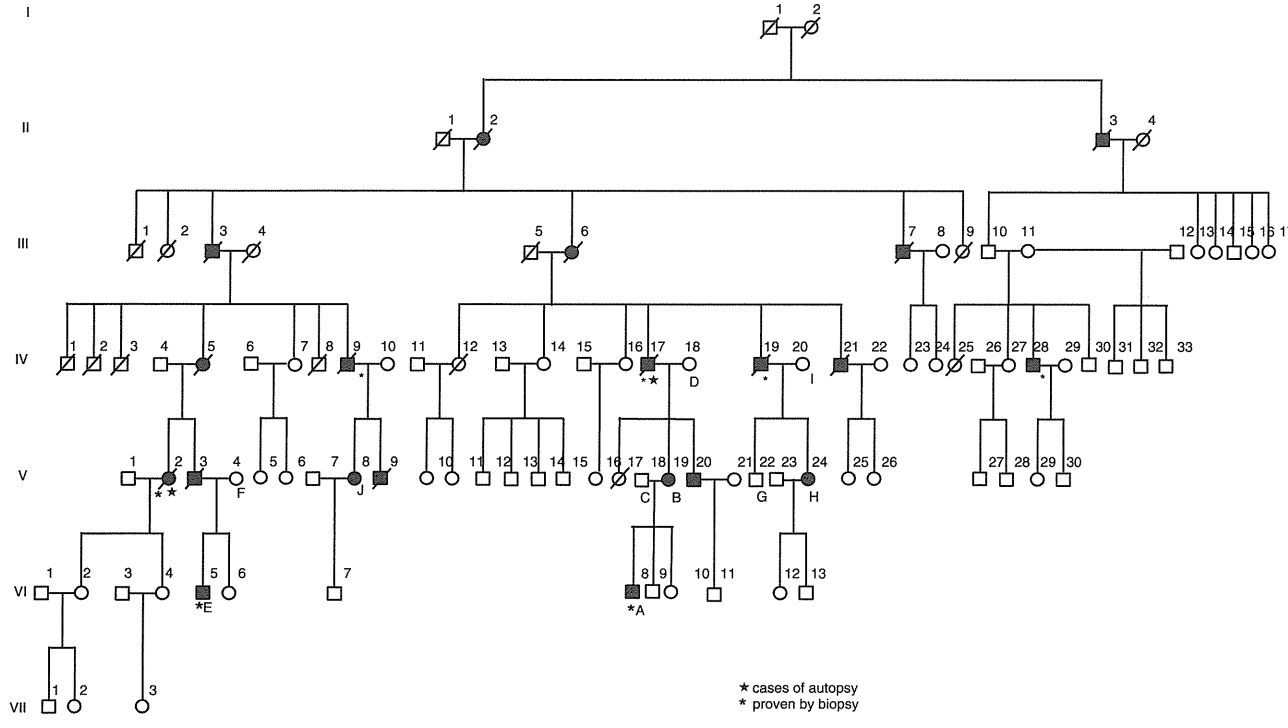

Figure 1 Family pedigree. Filled-in symbols indicate individuals with MFM. Empty symbols indicate unaffected individuals. A star and asterisk indicate autopsy-proven and muscle biopsy-proven cases, respectively. (A–J) indicates individuals whose DNA was used for this study.

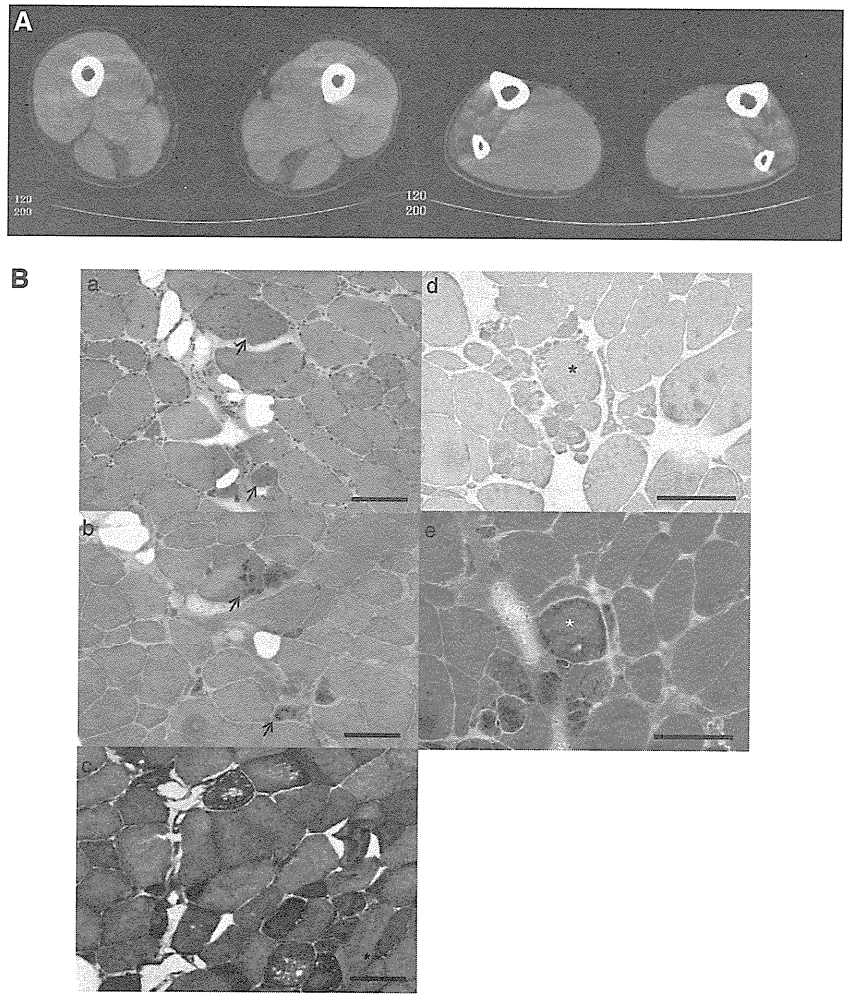

Figure 2 Family clinical data. (**A**) Muscle computed tomography of affected lower extremity. The imaging in the initial assessment of individual A showed symmetrical atrophy and fatty replacement of the semitendinosus in the proximal lower extremities (left) and the tibialis anterior, tibialis posterior, extensor hallucis and digitorum longus, and peroneal muscle in the distal (right) lower extremities. (**B**) Pathology of muscle biopsy. Hematoxylin-eosin (a), Gomori-trichrome (b) and NADH (nicotinamide adenine dinucleotide)-tetrazolium reductase (c) staining of the muscle biopsy sample from the tibialis anterior of individual E are shown. CBs are indicated by arrows. CBs were round or oval, 5–10 μm in diameter and predominantly located in the periphery of type 1 fibers, which stained eosinophilic with hematoxylin-eosin and blue–purple with Gomori-trichrome. NADH-tetrazolium reductase staining showed disorganization of the myofibrillar network. Immunostaining for desmin (d) and Gomori-trichrome staining (e) are serial sections of the muscle biopsy from individual E. Stars indicate corresponding fibers. No strong immunoreaction of desmin was seen in the CBs. Scale bars = 100 μm

homozygous for the alternative allele. After this first analysis, a second analysis was performed with all SNPs fulfilling the above criteria around the peaks identified in the first analysis.

Exome sequencing

Exome sequencing was performed on seven family members in three generations (A–E, H and I in Figure 1), four of whom were affected. Exon capture was performed with the SureSelect Human All Exon kit v2 (individuals E, H and I) or v4 (A–D) (Agilent Technologies, Santa Clara, CA, USA). Exon libraries were sequenced with the Illumina Hiseq 2000 platform according to the manufacturer's instructions (Illumina). Paired 101-base pair reads were aligned to the reference human genome (UCSChg19) using the Burrows-Wheeler Alignment tool.[7] Likely PCR duplicates were removed with the Picard program (http://picard.sourceforge.net/). Single-nucleotide variants and indels were identified using the Genome Analysis Tool Kit (GATK) v1.5 software.[8] SNVs and indels were annotated against the RefSeq database and dbSNP135 with the ANNOVAR program.[9] We used the PolyPhen2 polymorphism phenotyping software tool[10] to predict the functional effects of mutations.

Sanger sequencing

To confirm that mutations identified by exome sequencing segregated with the disease, we performed direct sequencing. PCR was performed with the primers shown in Supplementary Table 1. PCR products were purified with a MultiScreen PCR plate (Millipore, Billerica, MA, USA) and sequenced using BigDye terminator v1.1 and a 3500xL genetic analyzer (Applied Biosystems, Carlsbad, CA, USA).

RESULTS

Linkage analysis

The first linkage analysis identified five regions across autosomes with a logarithm of odds (LOD) score greater than 2 (Figure 3). Of the five regions, two were on chromosome 2 (from 167 cM to 168 cM, with a maximum LOD score of 2.46 and from 182 cM to 185 cM, with a maximum LOD score of 2.71), the other two were on chromosome 8 (from 27 cM to 34 cM, with a maximum LOD score of 2.71 and at 61 cM, with a maximum LOD score of 2.03), and one was on

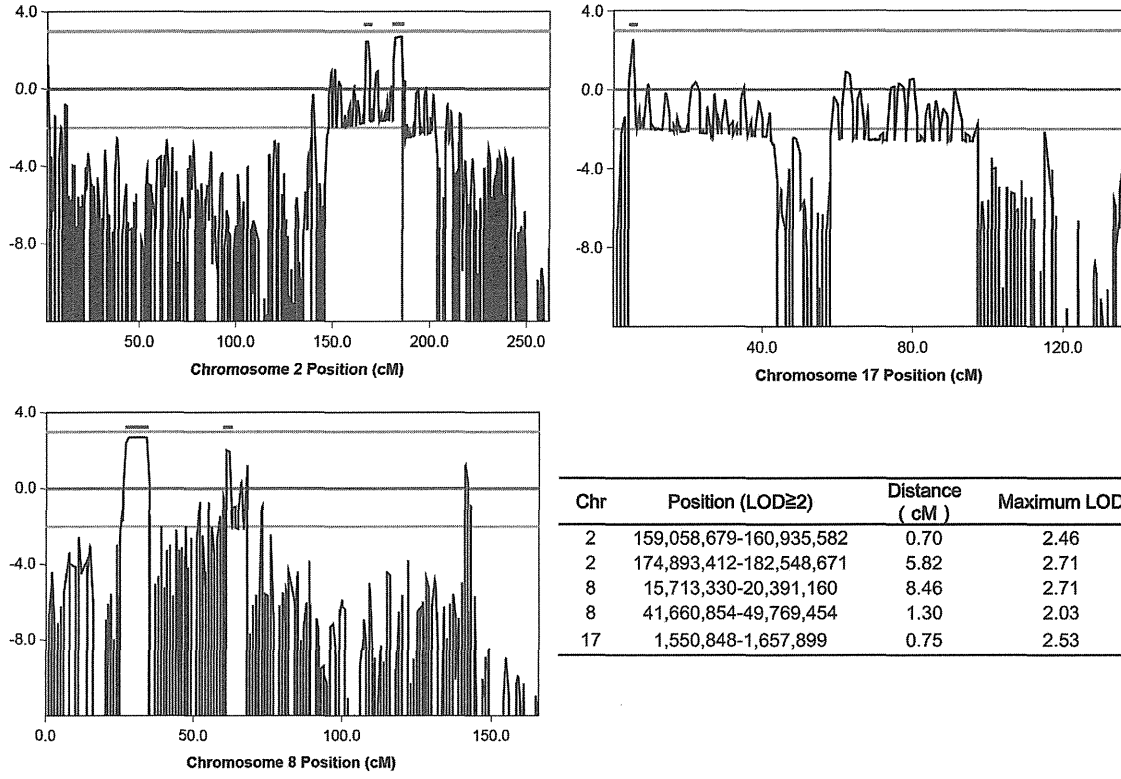

Chr	Position (LOD≧2)	Distance (cM)	Maximum LOD
2	159,058,679-160,935,582	0.70	2.46
2	174,893,412-182,548,671	5.82	2.71
8	15,713,330-20,391,160	8.46	2.71
8	41,660,854-49,769,454	1.30	2.03
17	1,550,848-1,657,899	0.75	2.53

Figure 3 Linkage analysis. Linkage analysis was performed on nine family members (four of them were affected, the others were unaffected) using an Illumina Human Omni 2.5 BeadChip. Five regions with an LOD score greater than 2 (indicated by bar) were identified. A full color version of this figure is available at the *Journal of Human Genetics* journal online.

Table 1 Summary of detected variants by exome sequencing

Individual *Morbidity*	*A* *Affected*	*B* *Affected*	*C* *Unaffected*	*D* *Unaffected*	*E* *Affected*	*H* *Affected*	*I* *Unaffected*	*Segregated in seven family members*
Exonic, splicing	10089	10064	10079	10065	10230	10194	10216	64
Nonsynonymous, splicing, indel, nonsense	4987	5020	5055	5038	5143	5234	5200	32
Allele frequency not available	577	600	536	555	671	794	786	2

chromosome 17 (at 5 cM, with a maximum LOD score of 2.53). In the second detailed linkage analysis, these peaks were determined to range from 167.49 cM at rs4233674 at position 159 058 679 to 168.19 cM at rs7598162 at position 160 935 582, and from 181.23 cM at rs4402725 at position 174 893 412 to 187.05 cM at rs7420169 at position 182 548 671 on chromosome 2; from 26.42 cM at rs2736043 at position 15 713 330 to 34.88 cM at rs9325871 at position 20 391 160, and from 61.02 cM at rs6999814 at position 41 660 854 to 62.32 cM at rs10957281 at position 49 769 454 on chromosome 8; and from 4.7 cM at rs11078552 at position 1 550 848 to 5.45 cM at rs1057355 at position 1 657 899 on chromosome 17. Haplotypes shared by affected individuals in these regions were confirmed by visual inspection. There were a few incompatible SNPs in these regions, presumably due to genotyping error.

Exome sequencing and segregation analysis

In exome sequencing, an average of 215 million reads enriched by SureSelect v4 (SSv4) and 319 million reads enriched by SureSelect v2 (SSv2) were generated, and 99% of reads were mapped to the reference genome by Burrows-Wheeler Alignment tool. An average of 57% (SSv4) and 61% (SSv2) of those reads were duplicated and removed, and an average of 80% (SSv4) and 66% (SSv2) of mapped reads without duplicates were in target regions. The average coverage of each exome was 163-fold (SSv4) and 130-fold (SSv2). An average of 85% (SSv4) and 69% (SSv2) of target regions were covered at least 50-fold (Supplementary Table 2). On average, 10 133 SNVs or indels, which are located within coding exons or splice sites, were identified per individual (Table 1). A total of 64 variants were common among patients and not present in unaffected individuals, and 32 of those were left after excluding synonymous SNVs. In these variants, only the heterozygous mutation c.90263G>T (NM_001256850) at position 179 410 777 of chromosome 2, which was predicted to p.W30088L in *TTN*, was novel (that is, not present in dbSNP v135 or 1000 genomes). Polyphen2 predicted this mutation as probably damaging. This mutation was located in a candidate region suggested by the linkage analysis in the present study. The other variants were registered with dbSNP135, and the allele frequencies, except for one SNV, rs138183879, in *IKBKB*, ranged from 0.0023 to 0.62.

a

Gene	Chr	Position	Variant type	Reference	Variant	dbSNP v135	Coding change	Prediction	Segregaion analysis
TTN	2	179 410777	Missense	G	T	Not present	W30088L	Probably damaging	Segregating
IKBKB	8	42 188 457	Missense	C	T	rs138183879	T742M	Benign	Non-segregating

b

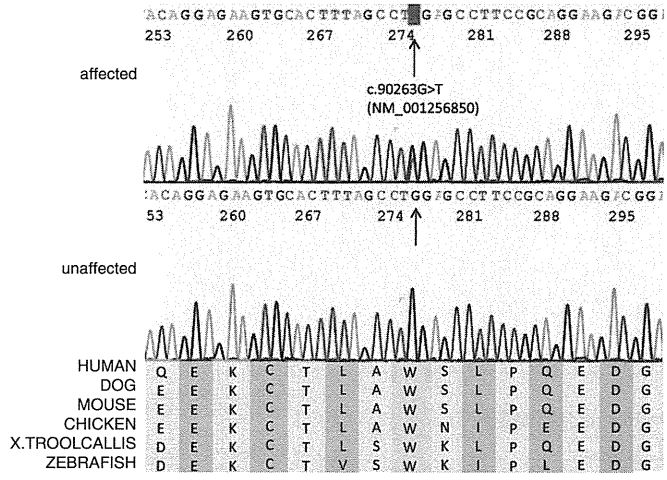

Figure 4 Identified mutations by exome sequencing. (**a**) We performed segregation analysis of two candidates. (**b**) The identified *TTN* mutation and its conservation among species. Sanger sequencing confirmed the heterozygous G to T substitution (indicated by the arrow) at the position chr2;179 410 777, which corresponds to c.90263G>T in exon 293 (NM_001256850.1). The substitution leads to p.W30088L (NP_001243779.1), and this amino acid is conserved among species.

These values were not compatible with the assumption that MFM was a rare disease and showed complete penetrance in this family. The allele frequency of rs138183879 was not available in dbSNP135, and this SNV was in the candidate region on chromosome 8 based on linkage analysis.

We then performed a segregation analysis on the two candidates, the novel mutation c.90263G>T in *TTN* and rs138183879 in *IKBKB*, through Sanger sequencing in 10 family members (A–J in Figure 1; Figure 4a). The rs138183879 SNP was not found in individual J, that is, it was not segregated with the disease in this family. In contrast, the novel mutation c.90263G>T in *TTN* was detected in all patients ($n=5$) and not detected in any of the unaffected family members ($n=5$) or 191 ethnically matched control subjects (382 chromosomes). These results suggested that this rare mutation in *TTN* segregated with the disease in this family.

DISCUSSION

In this study, we found that a novel missense mutation in *TTN* segregated with MFM in a large Japanese family. The identified c.90263G>T mutation in *TTN* (NM_001256850) was considered to be the genetic cause of MFM in our family, because (1) exome sequencing revealed that this was the best candidate mutation after filtering SNPs and indels, (2) this mutation is located in a region on chromosome 2 shared by affected family members, (3) the segregation with MFM was confirmed by Sanger sequencing, (4) this mutation was not detected in 191 control individuals, (5) this mutation was predicted to alter highly conserved amino acids (Figure 4b) and (6) *TTN* encodes a Z-disc-binding molecule called titin, which is similar to all of the previously identified causative genes for MFMs, which also encode Z-disc-associated molecules.

Recently, three mutations in *TTN* have been reported as the causes of hereditary myopathy with early respiratory failure (HMERF, MIM #603689),[11–16] which has similar muscle pathology to MFMs. The identified novel missense mutation c.90263G>T in our study was located on the same exon as recently reported HMERF mutations: c.90272C>T in a Portuguese family[16] and c.90315T>C in Swedish and English families[14,15] (Table 2). This finding suggests the possibility that our family can be recognized as having HMERF from a clinical aspect.

Compared with symptoms described in the past three reports on HMERF (also see Table 2), our patients have common features, such as autosomal dominant inheritance, early respiratory failure, the absence of clinically apparent cardiomyopathy, normal to mild elevation of serum CK and histological findings compatible with MFM. Early involvement of the tibialis anterior is also common, except for the Portuguese family, who reported isolated respiratory insufficiency and a milder presentation of HMERF. Thus, our family shares major clinical manifestations with patients with HMERF, suggesting that the identified mutation is novel for MFM and HMERF.

To date, mutations in *TTN* have been identified in skeletal myopathy and cardiomyopathy.[17,18] The relationship between the variant positions on *TTN* and phenotypes accompanied by skeletal or respiratory muscle involvement is summarized in Table 2. Titin is a large protein (4.20 MDa) that extends from the Z-disk to the M-line within the sarcomere, and it is composed of four major domains: Z-disc, I-band, A-band and M-line (Figure 5). All four HMERF mutations detected by other groups and our study were consistently located in the A-band domain, while mutations in tibial muscular dystrophy (TMD) (MIM #600334),[19–24] limb-girdle muscular dystrophy type 2J (LGMD2J) (#608807)[19,25] and early-onset myopathy with fatal cardiomyopathy (#611705)[26] were located in the M-line domain. HMERF and TMD have some common clinical characteristics, such as autosomal dominant inheritance with onset in adulthood and strong involvement of the tibialis anterior muscle.

Table 2 Previously reported TTN mutations with skeletal and/or respiratory muscle involvement

Phenotype	*LGMD*	*HMERF*	*Our family*	*HMERF*	*HMERF*	*TMD*	*TMD*	*LGMD2J*	*TMD*	*TMD*	*TMD*	*TMD*	*TMD*	*Early-onset myopathy with fatal cardiomyopathy*	*Early-onset myopathy with fatal cardiomyopathy*
Reported by	Vasli *et al.*[16]	Ohlsson *et al.*,[14] Pfeffer *et al.*[15]	Abe *et al.*[5]	Vasli *et al.*[16]	Edstrom *et al.*,[12] Nicolao, *et al.*[11] Lang e *et al.*[13]	Hackman *et al.*[23]	Udd *et al.*,[20] Hackman *et al.*[19]	Udd *et al.*,[25] Hackman *et al.*[19]	Pollazzon *et al.*[24]	Van den Bergh *et al.*[22]	Seze *et al.*,[21] Hackman *et al.*[19]	Hackman *et al.*[23]	Hackman *et al.*[23]	Carmignac *et al.*[26]	Carmignac *et al.*[26]
Mutation identified in Nucleotide (NM_001256850.1)	2012 c.3100G>A, c.52024G>A	2012 c.90315T>C	2012 c.90263G>T	2012 c.90272C>T	2005 c.97348C>T	2008 c.102724delT	2002 102857_102867 del11ins11	2002 102857_102867 del11ins11	2010 c.102914A>C	2003 c.102917T>A	2002 c.102944T>C	2008 c.102966delA	2008 c.102967C>T	2007 g.289385del ACCAAGTG	2007 g.291297delA
Protein (NP_001243779.1)	p.V1034M, p.A17342T	p.C30071R	p.W30088L	p.P30091L	p.R32450W				p.H34305P	p.I34306N	p.L34315P		p.Q34323X		
Domain	I-band, A-band	A-band (Fn3)	A-band (Fn3)	A-band (Fn3)	A-band (kinase)	M-line	M-line	M-line	M-line	M-line	M-line	M-line	M-line	M-line	M-line
Population	French	Swedish English	Japanese	Portuguese	Swedish	French	Finnish	Finnish	Italian	Belgian	French	Spanish	French	Sudanese	Moroccan
Inheritance	AR	AD	AD	AD	AD	AD	AD	AR	AD	AD	AD	AD	AD	Consanguineous siblings	Consanguineous siblings
Onset	35	33–71	27–45	46	20–50s	20–30s	35–55	20–30s	50–60s	47	45	40–50s	30s	Neonatal	Infant-early childhood
Skeletal muscles															
Major	Proximal UL and LL	TA, PL, EDL, ST	TA, ST	No	TA, neck flexor, proximals	TA, GA,HAM, pelvic	TA	All proximals	TA	TA	TA	TA	TA, HAM, pelvic	General muscle weakness and hypotonia	Psoas, TA, GA, peroneus
Minor		Neck flexor	Cervical, shoulder girdles, intercostals, proximal limb			QF				EDL, peroneal, TP	GA, femoral, scapular	HAM, GA	GA, distal UL		QF, proximal UL, neck, facial, trunk flexor
Spared			Facial			Proximal UL	Facial, UL, proximals	Facial		UL, proximal LL	Facial	UL	Proximal UL, QF		
Cardiac muscles	ND	No	No	ND	ND	ND	No	No	ND	ND	ND	ND	ND	DCM, onset; in the first decade	DCM, onset; 5–12 years old
Respiratory failure	ND	Yes, within 5–8 years	Yes, within 7 years	Isolated respiratory failure	Yes, as first presentation	ND	ND	ND	ND	ND	ND	ND	ND	ND	ND
Muscle pathologic features	ND	Inclusion bodies (major) and RVs (minor)	Cytoplasmic bodies (major) and RVs (minor)	Cytoplasmic bodies	Cytoplasmic bodies, positive for rhodamine-conjugated phalloidin	Dystrophic pattern without vacuoles	Nonspecific dystrophic change	Nonspecific dystrophic change, loss of calpain-3	Dystrophic pattern with RVs	Nonspecific, RV	Nonspecific	Dystrophic pattern with RVs	Nonspecific	Minicore-like lesions and abundant central nuclei	Minicore-like lesions and abundant central nuclei

Abbreviations: AD, autosomal dominant; AR, autosomal recessive; DCM, dilated cardiomyopathy; EDL, extensor digitorum longus; GA, gastrocnemius; HAM, hamstrings; LL, lower limb; ND, not described; no, no involvement; PL, peroneus longus; QF, quadriceps femoris; RV, rimmed vacuole;
ST, semitendinosus; TA, tibialis anterior; TMD, tibial muscular dystrophy; TP, tibialis posterior; UL, upper limb.

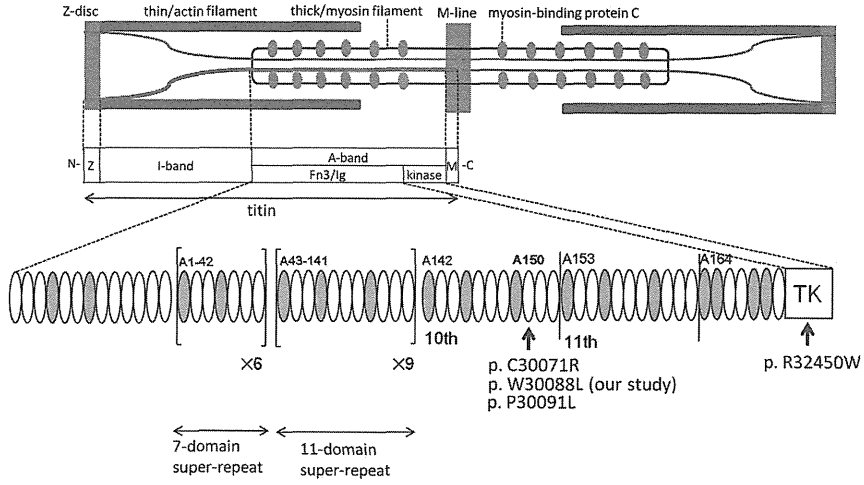

Figure 5 Structure of titin and mutation distribution in the A-band domain. Human *TTN* was mapped to 2q31.2. *TTN* is 294 kb and is composed of 363 exons that code for a maximum of 38 138 amino-acid residues and a 4.20-MDa protein[32] called titin. Titin is expressed in the cardiac and skeletal muscles and spans half the sarcomere, with its N-terminal at the Z-disc and the C-terminal at the M-line.[33] Titin is composed of four major domains: Z-disc, I-band, A-band and M-line. I-band regions of titin are thought to make elastic connections between the thick filament (that is, myosin filament) and the Z-disc within the sarcomere, whereas the A-band domain of titin seems to be bound to the thick filament, where it may regulate filament length and assembly.[34] The gray and white ellipses indicate an Ig-like domain and fibronectin type 3 domain, respectively. Our mutation (p.W30088L) and the neighboring two mutations (that is, p.C30071R and p.P30091L) were all located in the 6th Fn3 domain in the 10th domain of large super-repeats. A full color version of this figure is available at the *Journal of Human Genetics* journal online.

In contrast, one of the distinctive features of TMD is that early respiratory failure has not been observed in patients with TMD. Histological findings of TMD usually do not include CBs but show nonspecific dystrophic change. The underlying pathogenic processes explaining why mutations on these neighboring domains share some similarities but also some differences are unknown.

Three of four HMERF mutations in the A-band domain are located in the fibronectin type 3 and Ig-like (Fn3/Ig) domain, and one of four HMERF mutations is located in the kinase domain (Table 2, also see Figure 5). The missense mutation c.97348C>T in the kinase domain was the first reported HMERF mutation. It has been shown that the kinase domain has an important role in controlling muscle gene expression and protein turnover via the neighbor of BRCA1 gene-1-muscle-specific RING finger protein-serum response transcription factor pathway.[13] Moreover, the Fn3/Ig domain is composed of two types of super-repeats: six consecutive copies of 7-domain super-repeat at the N-terminus and 11 consecutive copies of 11-domain super-repeat at the C-terminus.[27–29] These super-repeats are highly conserved among species and muscles. Our identified mutation (c.90263G>T) and the neighboring two mutations (that is, c.90272C>T and c.90315T>C shown in Table 2) were all located on the 6th Fn3 domain in the 10th copy of 11-domain super-repeat (that is, A150 domain[30]) (Figure 5). Although some Fn3 domains are proposed to be the putative binding site for myosin,[31] the role with the majority of Fn3 domains, how it supports the structure of each repeat architecture, and the identity of its binding partner have not been fully elucidated. Our findings suggested that the Fn3 domain, in which mutations clustered, has critical roles in the pathogenesis of HMERF, although detailed mechanisms of pathogenesis remain unknown.

In conclusion, we have identified a novel disease-causing mutation in *TTN* in a family with MFM that was clinically compatible with HMERF. Because of its large size, global mutation screening of *TTN* has been difficult. Mutations in *TTN* may be detected by massively parallel sequencing in more patients with MFMs, especially in patients with early respiratory failure. Further studies are needed to understand the genotype–phenotype correlations in patients with mutations in *TTN* and the molecular function of titin.

ACKNOWLEDGEMENTS

We thank the patients and their family. We are grateful to Yoko Tateda, Kumi Kato, Naoko Shimakura, Risa Ando, Riyo Takahashi, Miyuki Tsuda, Nozomi Koshita, Mami Kikuchi and Kiyotaka Kuroda for their technical assistance. We also acknowledge the support of the Biomedical Research Core of Tohoku University Graduate School of Medicine. This work was supported by a grant of Research on Applying Health Technology provided by the Ministry of Health, Labor and Welfare to YM, an Intramural Research Grant (23-5) for Neurological and Psychiatric Disorders of NCNP and JSPS KAKENHI Grant number 24659421.

1 Nakano, S., Engel, A. G., Waclawik, A. J., Emslie-Smith, A. M. & Busis, N. A. Myofibrillar myopathy with abnormal foci of desmin positivity. I. Light and electron microscopy analysis of 10 cases. *J. Neuropathol. Exp. Neurol.* **55,** 549–562 (1996).
2 Olive, M., Odgerel, Z., Martinez, A., Poza, J. J., Bragado, F. G., Zabalza, R. J. *et al.* Clinical and myopathological evaluation of early- and late-onset subtypes of myofibrillar myopathy. *Neuromuscul. Disord.* **21,** 533–542 (2011).
3 Olive, M., Goldfarb, L. G., Shatunov, A., Fischer, D. & Ferrer, I. Myotilinopathy: refining the clinical and myopathological phenotype. *Brain* **128,** 2315–2326 (2005).
4 Selcen, D. & Engel, A. G. Myofibrillar myopathy caused by novel dominant negative alpha B-crystallin mutations. *Ann. Neurol.* **54,** 804–810 (2003).
5 Abe, K., Kobayashi, K., Chida, K., Kimura, N. & Kogure, K. Dominantly inherited cytoplasmic body myopathy in a Japanese kindred. *Tohoku. J. Exp. Med.* **170,** 261–272 (1993).
6 Abecasis, G. R., Cherny, S. S., Cookson, W. O. & Cardon, L. R. Merlin–rapid analysis of dense genetic maps using sparse gene flow trees. *Nat. Genet.* **30,** 97–101 (2002).
7 Li, H. & Durbin, R. Fast and accurate short read alignment with Burrows-Wheeler transform. *Bioinformatics* **25,** 1754–1760 (2009).
8 McKenna, A., Hanna, M., Banks, E., Sivachenko, A., Cibulskis, K., Kernytsky, A. *et al.* The Genome Analysis Toolkit: a MapReduce framework for analyzing next-generation DNA sequencing data. *Genome. Res.* **20,** 1297–1303 (2010).
9 Wang, K., Li, M. & Hakonarson, H. ANNOVAR: functional annotation of genetic variants from high-throughput sequencing data.. *Nucleic Acids Res.* **38,** e164 (2010).
10 Adzhubei, I. A., Schmidt, S., Peshkin, L., Ramensky, V. E., Gerasimova, A., Bork, P. *et al.* A method and server for predicting damaging missense mutations. *Nat. Methods* **7,** 248–249 (2010).
11 Nicolao, P., Xiang, F., Gunnarsson, L. G., Giometto, B., Edstrom, L., Anvret, M. *et al.* Autosomal dominant myopathy with proximal weakness and early respiratory muscle involvement maps to chromosome 2q. *Am. J. Hum. Genet.* **64,** 788–792 (1999).

12 Edstrom, L., Thornell, L. E., Albo, J., Landin, S. & Samuelsson, M. Myopathy with respiratory failure and typical myofibrillar lesions. *J. Neurol. Sci.* **96,** 211–228 (1990).
13 Lange, S., Xiang, F., Yakovenko, A., Vihola, A., Hackman, P., Rostkova, E. *et al.* The kinase domain of titin controls muscle gene expression and protein turnover. *Science* **308,** 1599–1603 (2005).
14 Ohlsson, M., Hedberg, C., Bradvik, B., Lindberg, C., Tajsharghi, H., Danielsson, O. *et al.* Hereditary myopathy with early respiratory failure associated with a mutation in A-band titin. *Brain* **135,** 1682–1694 (2012).
15 Pfeffer, G., Elliott, H. R., Griffin, H., Barresi, R., Miller, J., Marsh, J. *et al.* Titin mutation segregates with hereditary myopathy with early respiratory failure. *Brain* **135,** 1695–1713 (2012).
16 Vasli, N., Bohm, J., Le Gras, S., Muller, J., Pizot, C., Jost, B. *et al.* Next generation sequencing for molecular diagnosis of neuromuscular diseases. *Acta. Neuropathol.* **124,** 273–283 (2012).
17 Kontrogianni-Konstantopoulos, A., Ackermann, M. A., Bowman, A. L., Yap, S. V. & Bloch, R. J. Muscle giants: molecular scaffolds in sarcomerogenesis. *Physiol. Rev.* **89,** 1217–1267 (2009).
18 Ottenheijm, C. A. & Granzier, H. Role of titin in skeletal muscle function and disease. *Adv. Exp. Med. Biol.* **682,** 105–122 (2010).
19 Hackman, P., Vihola, A., Haravuori, H., Marchand, S., Sarparanta, J., De Seze, J. *et al.* Tibial muscular dystrophy is a titinopathy caused by mutations in TTN, the gene encoding the giant skeletal-muscle protein titin. *Am. J. Hum. Genet.* **71,** 492–500 (2002).
20 Udd, B., Partanen, J., Halonen, P., Falck, B., Hakamies, L., Heikkila, H. *et al.* Tibial muscular dystrophy. Late adult-onset distal myopathy in 66 Finnish patients. *Arch. Neurol.* **50,** 604–608 (1993).
21 de Seze, J., Udd, B., Haravuori, H., Sablonniere, B., Maurage, C. A., Hurtevent, J. F. *et al.* The first European family with tibial muscular dystrophy outside the Finnish population. *Neurology* **51,** 1746–1748 (1998).
22 Van den Bergh, P. Y., Bouquiaux, O., Verellen, C., Marchand, S., Richard, I., Hackman, P. *et al.* Tibial muscular dystrophy in a Belgian family. *Ann. Neurol.* **54,** 248–251 (2003).
23 Hackman, P., Marchand, S., Sarparanta, J., Vihola, A., Penisson-Besnier, I., Eymard, B. *et al.* Truncating mutations in C-terminal titin may cause more severe tibial muscular dystrophy (TMD). *Neuromuscul. Disord.* **18,** 922–928 (2008).
24 Pollazzon, M., Suominen, T., Penttila, S., Malandrini, A., Carluccio, M. A., Mondelli, M. *et al.* The first Italian family with tibial muscular dystrophy caused by a novel titin mutation. *J. Neurol.* **257,** 575–579 (2010).
25 Udd, B., Rapola, J., Nokelainen, P., Arikawa, E. & Somer, H. Nonvacuolar myopathy in a large family with both late adult onset distal myopathy and severe proximal muscular dystrophy. *J. Neurol. Sci.* **113,** 214–221 (1992).
26 Carmignac, V., Salih, M. A., Quijano-Roy, S., Marchand, S., Al Rayess, M. M., Mukhtar, M. M. *et al.* C-terminal titin deletions cause a novel early-onset myopathy with fatal cardiomyopathy. *Ann. Neurol.* **61,** 340–351 (2007).
27 Labeit, S., Barlow, D. P., Gautel, M., Gibson, T., Holt, J., Hsieh, C. L. *et al.* A regular pattern of two types of 100-residue motif in the sequence of titin. *Nature* **345,** 273–276 (1990).
28 Labeit, S. & Kolmerer, B. Titins: giant proteins in charge of muscle ultrastructure and elasticity. *Science* **270,** 293–296 (1995).
29 Tskhovrebova, L., Walker, M. L., Grossmann, J. G., Khan, G. N., Baron, A. & Trinick, J. Shape and flexibility in the titin 11-domain super-repeat. *J. Mol. Biol.* **397,** 1092–1105 (2010).
30 Bucher, R. M., Svergun, D. I., Muhle-Goll, C. & Mayans, O. The structure of the FnIII Tandem A77-A78 points to a periodically conserved architecture in the myosin-binding region of titin. *J. Mol. Biol.* **401,** 843–853 (2010).
31 Muhle-Goll, C., Habeck, M., Cazorla, O., Nilges, M., Labeit, S. & Granzier, H. Structural and functional studies of titin's fn3 modules reveal conserved surface patterns and binding to myosin S1–a possible role in the Frank-Starling mechanism of the heart. *J. Mol. Biol.* **313,** 431–447 (2001).
32 Bang, M. L., Centner, T., Fornoff, F., Geach, A. J., Gotthardt, M., McNabb, M. *et al.* The complete gene sequence of titin, expression of an unusual approximately 700-kDa titin isoform, and its interaction with obscurin identify a novel Z-line to I-band linking system. *Circ. Res.* **89,** 1065–1072 (2001).
33 Maruyama, K., Yoshioka, T., Higuchi, H., Ohashi, K., Kimura, S. & Natori, R. Connectin filaments link thick filaments and Z lines in frog skeletal muscle as revealed by immunoelectron microscopy. *J. Cell. Biol.* **101,** 2167–2172 (1985).
34 Guo, W., Bharmal, S. J., Esbona, K. & Greaser, M. L. Titin diversity–alternative splicing gone wild. *J. Biomed. Biotechnol.* **2010,** 753675 (2010).

Supplementary Information accompanies the paper on Journal of Human Genetics website (http://www.nature.com/jhg)

Edited by Jeffrey L. Noebels, Massimo Avoli, Michael A. Rogawski, Richard W. Olsen, Antonio V. Delgado-Escueta
JASPER'S BASIC MECHANISMS OF THE EPILEPSIES
Fourth Edition
NCBI Bookshelf Online Book Version

Haploinsufficiency of *STXBP1* and Ohtahara syndrome

Hirotomo Saitsu[1]

Mitsuhiro Kato[2]

Naomichi Matsumoto[1]

[1] *Department of Human Genetics, Yokohama City University Graduate School of Medicine*
[2] *Department of Pediatrics, Yamagata University Faculty of Medicine*

Abstract

Ohtahara syndrome (OS) is one of the most severe and earliest forms of epilepsy. Brain malformations or metabolic disorders are often associated with OS, but other cases remain etiologically unexplained. Here we show that *de novo* heterozygous mutations in the gene encoding STXBP1, also known as MUNC18-1, which is essential in synaptic vesicle release in multiple species, cause OS. A microdeletion involving *STXBP1* and various point mutations, including missense, frameshift, nonsense, and splicing mutations, have been found in individuals with OS. Transcripts associated with frameshift, nonsense, and splicing mutations are likely to be degraded by nonsense mediated mRNA decay. Moreover, STXBP1 proteins harboring missense mutations were unstable compared with the wild-type, and were degraded in Neuroblastoma2A cells. Binding of a mutant protein (p.C180Y) to syntaxin-1A was also significantly impaired. These findings strongly suggest that haploinsufficiency of *STXBP1* causes OS. Mutations of *STXBP1* also suggest that aberrations of genes involved in synaptic vesicle release might be associated with other types of infantile epilepsy.

Brief introduction

Ohtahara syndrome (OS), also known as early infantile epileptic encephalopathy with suppression-burst, is one of the most severe and earliest forms of epilepsy.[1] It is characterized by early onset of tonic seizures, seizure intractability, characteristic suppression-burst patterns on the electroencephalogram (EEG), and a poor outcome with severe psychomotor retardation.[2,3] Brain malformations, such as cerebral dysgenesis or hemimegalencephaly, are often associated with OS, but cryptogenic or idiopathic OS is found in a subset of OS patients, in whom genetic aberrations might be involved.[4] Although mutations of the *ARX* gene have been found in several male patients with OS,[5–8] the genetic causes are unexplained in most cryptogenic OS cases. We have recently found *de novo* mutations in *STXBP1* (encoding syntaxin binding protein 1, also known as MUNC18-1) in individuals with cryptogenic OS.[9] Here we present all the mutations in *STXBP1* found to date in OS patients, as well as some evidence of mutations leading to haploinsufficiency.

OHTAHARA SYNDROME

Ohtahara syndrome was first reported as the earliest form of age-dependent epileptic syndromes by Ohtahara et al.[1] It is characterized by early onset of intractable tonic spasms, characteristic suppression-burst patterns on interictal EEG, and a poor outcome with severe psychomotor retardation.[2,3] According to a previous report,[4] all patients have seizure onset

Address correspondence to: Dr. Hirotomo Saitsu, Department of Human Genetics, Yokohama City University Graduate School of Medicine, 3-9 Fukuura, Kanazawa-ku, Yokohama 236-0004, Japan. Tel.: +81-45-787-2606, Fax: +81-45-786-5219, E-mail: hsaitsu@yokohama-cu.ac.jp.

within the first 3 months, with the majority (75%) in the first month. Tonic spasms were observed in all patients. One-third to one-half of patients also had partial seizures, such as erratic focal motor seizures and hemiconvulsions, or asymmetric tonic seizures; however, myoclonic seizures were rare. Hemiconvulsions, tonic seizures, or clonic seizures precede the onset of tonic spasms by 1 to several weeks to in 37.5% of OS patients.[4] Brain malformations, such as cerebral dysgenesis, hemimegalencephaly, porencephaly, and Aicardi syndrome are often associated with OS, but a significant proportion of patients (31% to 50% of OS cases) remain etiologically unexplained.[2,4] Suppression-burst patterns on interictal EEG consisting of high-voltage activity alternating with nearly flat suppression phases are observed when the patient is both awake and asleep.

Early myoclonic encephalopathy (EME) is another epileptic syndrome showing suppression-burst patterns on EEG.[10] The prevailing initial seizure type is a main difference between OS and EME: tonic seizures in OS and myoclonic seizures in EME.[2,3] However, OS and EME have common features, and it is often difficult to distinguish between them. Homozygous missense mutations of the *SLC25A22* (mitochondrial glutamate carrier 1) gene have been recently found in EME individuals in consanguineous familes.[11,12] Age-dependent evolution is a characteristic feature of both OS and EME: approximately 75% and 40 % of OS and EME cases transit to West syndrome (WS) usually 3–4 months afterwards.[2,3] West syndrome is characterized by tonic spasms with clustering, arrest of psychomotor development, and hypsarrhythmia on EEG. Such transitions suggest a common pathophysiology between OS and WS or between EME and WS. Consistent with this hypothesis, specific mutations of the *ARX* (*aristaless*-related homeobox) gene at Xp22.13, have been recently found in male OS and WS cases.[5–8,13–15]

DE NOVO STXBP1 MUTATIONS CAUSE OS

Identification of *STXBP1* Mutations in Patients with OS

Through BAC array-based comparative genomic hybridization analysis of patients associated with mental retardation (MR), we found a microdeletion at 9q33.3-q34.11 in a female patient with OS.[9] As the microdeletion occurred *de novo*, we assumed that a gene within the deletion was responsible for OS. Among the genes mapped within the deletion, the gene encoding syntaxin binding protein 1 (STXBP1,) was of particular interest because mouse *Stxbp1* has been shown to be essential for synaptic vesicle release[16] and is specifically expressed in the brains of rodents and humans.[17,18] We therefore analyzed *STXBP1* in 13 unrelated patients with OS. Four heterozygous missense mutations were found at evolutionary conserved amino acids in three males and one female (Figure 1 and Table 1). Three mutations were confirmed as *de novo* events (paternal DNA was unavailable for one remaining mutation).

Jasper's Basic Mechanisms of the Epilepsies

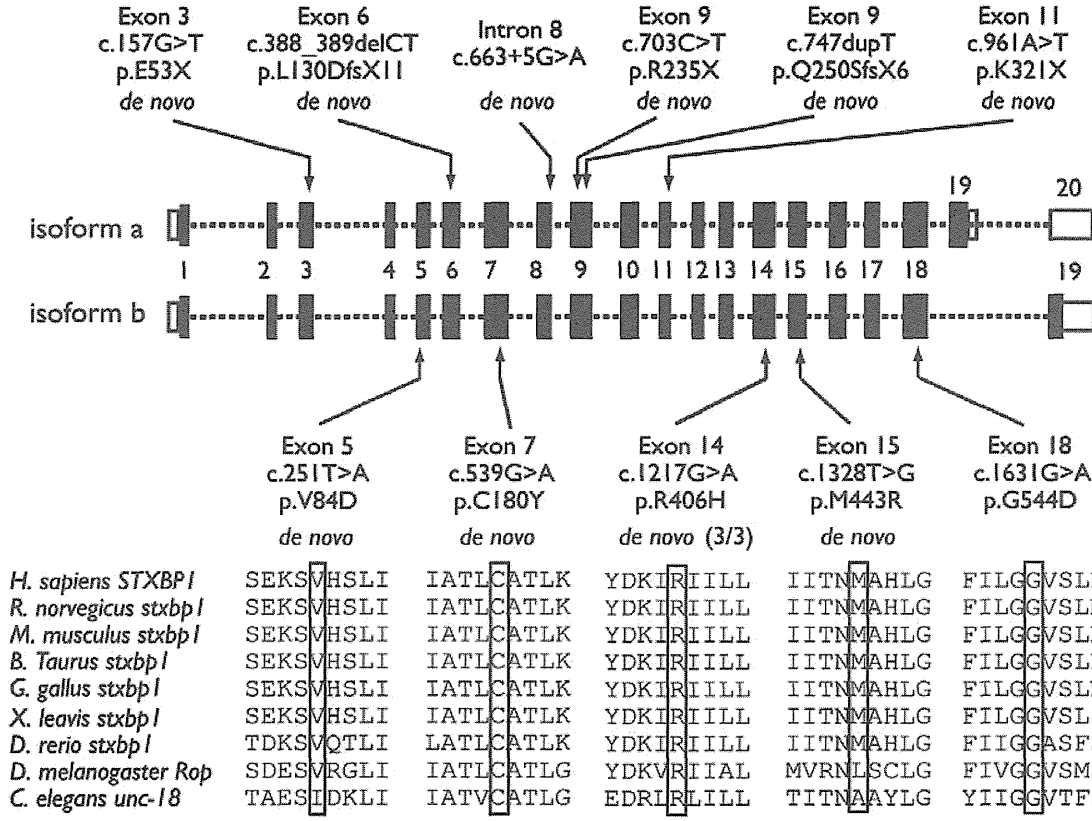

Figure 1. Summary of *STXBP1* mutations found in Japanese individuals with OS

Schematic representation of *STXBP1*, consisting of at most 20 exons (the UTR and the coding region are open and filled rectangles, respectively). There are two isoforms, **a** (GenBank accession number, NM_003165) with exon 19, and **b** (NM_001032221) without exon 19 of isoform **a**. Locations of mutations are indicated by arrows. Eleven different mutations are presented: missense mutations are indicated below the gene scheme, and the other types of mutations are indicated above the gene. Ten mutations in 12 subjects occurred *de novo*. All missense mutations occurred at conserved amino acids. CLUSTALW (http://align.genome.jp/) was used to align homologs of different species. Adapted from Refs.[9] and [19]

Table 1
Summary of Clinical Features of Subjects with *STXBP1* Deletion/Mutations

Case # Mutation	Initial Symptoms	Onset of Spasms	Transition from Spasms to Other Seizures	Response to Therapy
#1 Deletion	Tonic seizure and oral automatism	2 m	Generalized clonic seizure at 29 m	Seizure free from 5m after TRH injection
#2 c.1631G>A	Blinking	10 d	No	Seizure free from 3m
#3 c.539G>A	Tonic seizure with blinking	3 m	No	Intractable, daily
#4 c.1328T>G	Upward gazing and tonic seizure	2 m	Partial seizure at 8 m	Intractable, hourly TRH injection was temporally effective
#5 c.251T>A	Spasms and tonic-clonic seizure	2 m	No	Intractable, daily
#6 c.1217G>A	Generalized convulsions	3 w	No	Intractable, hourly
#7 c.1217G>A	GTCS with upward eye gazing	2 m	Myoclonic seizure at 48 d	Intractable, daily
#8 .1217G>A	Partial seizures (right hemi convulsion)	2 m	Tonic seizure to myoclonic seizure	Intractable, daily
#9 c.157G>T	Spasms	2 d	Versive seizure after hypoxia at 2 y	Intractable, daily
#10 c.388_389del	Secondary generalized seizures	2 m	CPS	Seizure free after ACTH or VPA with KBr
#11 c.663+5G>A	Blinking to tonic seizures	1 m	Tonic seizure	Seizure free with VB6 for spasms and ACTH for WS
#12 c.703C>T	Spasms in cluster	1 m	No	Seizure free from 6 m after high-dose PB
#13 c.747dup	Clonic convulsion	31 d	Partial seizure and myoclonic seizures	Intractable, hourly
#14 c.961A>T	Partial seizures	3 w	Partial seizure	Intractable, daily

GTCS, generalized tonic-clonic seizures; CPS, complex partial seizure; TRH, thyrotropin-releasing hormone; ACTH, adrenocorticotropic hormone; VPA, valproic acid; KBr, Potassium bromide; VB_6, vitamin B6; PB, phenobarbital; d, day(s); w, week; m, month(s); y, year(s); 0 w, 0 to 6 days; 0 m, 0 to 3 weeks

STXBP1 Mutation Is a Major Genetic Cause of OS

To delineate the clinical spectrum of patients with *STXBP1* mutations, *STXBP1* was further analyzed in 29 and 54 cases of cryptogenic OS and WS, respectively.[19] No brain malformations were found in any of the cases. Seven novel heterozygous mutations were found in nine OS cases (the same mutation was found in three cases), but none in WS cases (six males and three females: Figure 1 and Table 1). The mutations included one missense, one splicing, two frameshift, and three nonsense mutations. A recurrent missense mutation (c.1217G>A, p.R406H) occurred at an evolutionarily conserved amino acid (Figure 1). All the mutations occurred *de novo*. Collectively, *STXBP1* aberrations account for about one-third of individuals

with OS (14 out of 43). These data showed that *STXBP1* mutations are a major genetic cause of cryptogenic OS, but they are not a genetic cause of WS in our Japanese cohort.

Clinical Features of Patients with *STXBP1* Deletion/Mutations

Clinical information from 14 individuals with confirmed *STXBP1* deletion/mutations is summarized in Table 1. These persons showed distinctive features of OS, such as early-onset seizures including epileptic spasms, suppression-burst pattern on EEG, transition to WS after a few to several months, and severe developmental delay. Epileptic spasms were preceded by other seizure types, including partial seizures in 11 subjects. Transition to WS was observed in 11 subjects with OS. Although seizures were intractable in nine subjects, five subjects responded to medication, such as thyrotropin-releasing hormone (TRH) injection, adrenocorticotropic hormone (ACTH) injection, vitamin B_6, high-dose phenobarbital, and valproic acid. All subjects demonstrated severe psychomotor developmental delay. Brain magnetic resonance imaging (MRI) showed no structural anomalies or hippocampal anomalies but did show some atrophy (Figure 2A). Suppression-burst on interictal EEG was observed in both awake and asleep states (Figure 2B). We gained several insights into the phenotype of *STXBP1* aberrations. Firstly, the age at onset of epileptic spasms is later in subjects with *STXBP1* aberrations than in the 16 original subjects reported by Yamatogi and Ohtahara.[4] Only 27 % of the subjects (4/15) in our series had onset of OS within 1 month compared to 75 % (12/16) in the series of Yamatogi and Ohtahara. As subjects with *STXBP1* aberrations showed no structural anomalies on brain MRI examination, the onset of epileptic seizures might be affected by associated structural brain abnormalities, which are commonly seen in other reports of OS. Secondly, myoclonic seizures, which are thought to be rarely observed in OS, were occasionally observed (3/14). Myoclonic seizures are the main ictal symptom of EME. These three subjects can be diagnosed as having EME when myoclonic seizures dominate. Thus, *STXBP1* might also be causative for EME, implying a genetic linkage between OS and EME. Another infrequent but interesting finding is that one patient (no.5) developed vigorous chorea–ballismus subsequent to OS, suggesting that mutations of *STXBP1* could affect the basal ganglia.[9,20] In terms of the genotype-phenotype relationship, we found no difference in clinical data between seven subjects with missense mutations and seven subjects with microdeletions, premature termination codons, or splicing mutations. This finding is supported by our experimental data that demonstrated both missense mutations and a splicing mutation resulted in haploinsufficiency of *STXBP1*: degradation of STXBP1 proteins containing missense mutations and nonsense-mediated mRNA decay (NMD) associated with aberrantly spliced mRNAs (see below).

Jasper's Basic Mechanisms of the Epilepsies

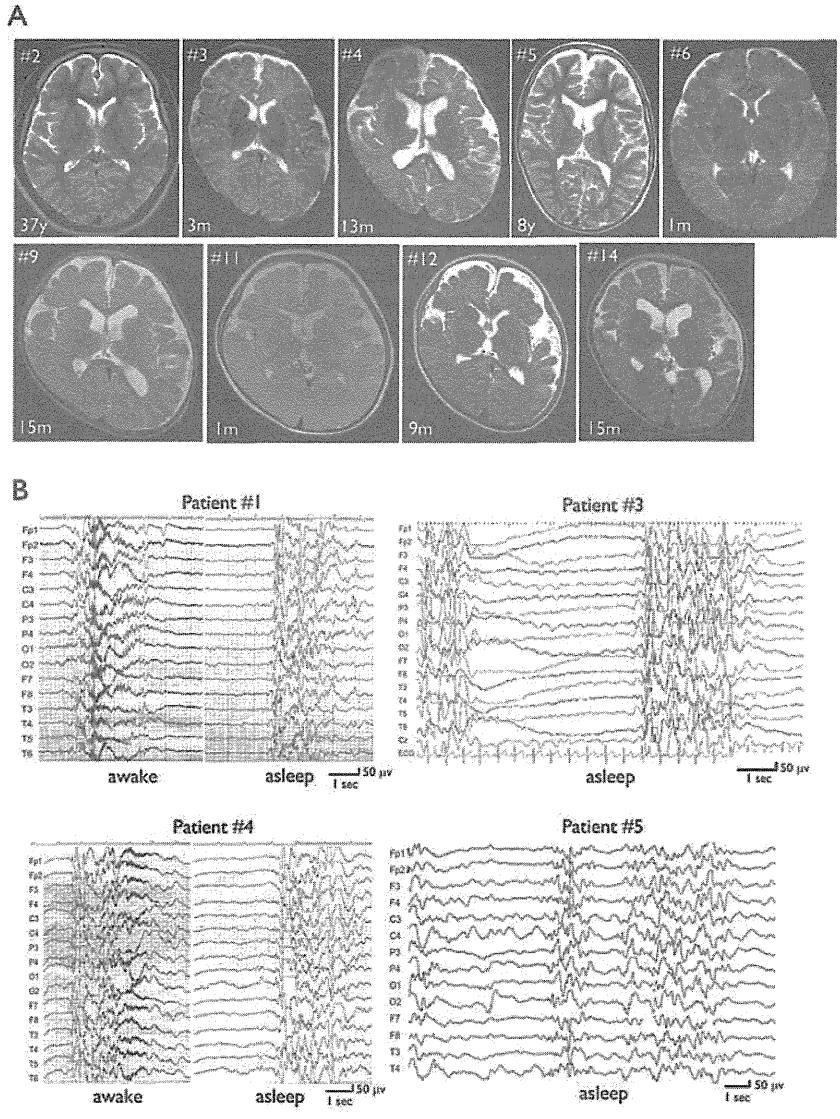

Figure 2. Brain MRI scan and EEG of OS patients with *STXBP1* aberrations

(A) Brain MRI (T2-weighted axial) image through the basal ganglia shows normal brain structure in patients with *STXBP1* mutations. Patient IDs and developmental stages are indicated. Mild dilatation of lateral ventricles is observed in patients #4, #9, #11, and #14, but none shows brain malformation. y, year(s); m, month(s). (B) Suppression-burst on interictal EEG of patients #1 (at age 2 months), #3 (at 3 months), #4 (at 2 months), and #5 (at 3 months). High-voltage bursts alternating with almost flat suppression phases at an approximately regular rate in both awake and asleep states. Adapted from Refs.[9] and [19]

MOLECULAR EVIDENCE OF *STXBP1* HAPLOINSUFFICIENCY

Mutant STXBP1 Proteins Are Unstable

All five missense mutations lead to amino acid replacements in the hydrophobic core of STXBP1 and are considered to destabilize the folding architecture. This is especially true for the three mutants (p.V84D, p.G544D and p.M443R) that have replaced the wild-type (WT) residues with charged residues, which would be predicted to severely disrupt the conformation of STXBP1.[9] In fact, circular dichroism (CD) spectra showed that the helical content of the C180Y mutant is lower (39%) than that of the WT (43%), suggesting that the mutation

destabilized the secondary structure of STXBP1 [9](Figure 3A). Moreover, CD melting experiments revealed that the melting temperature (T_m) of the C180Y mutant was about 11 degrees lower than that of the WT (Figure 3B), indicating that the C180Y mutant is much more unstable than the WT. The regulation of synaptic vesicle release by Stxbp1 is mediated in part by binding to Syntaxin-1A as well as directly to the Soluble N-ethylmaleimide-sensitive factor attachment protein receptor (SNARE) complex, which mediates fusion of vesicles with the target membrane.[21,22] Binding of a mutant protein (p.C180Y) to syntaxin-1A was also significantly impaired, even at 4 °C in vitro.[9] Together with the fact that the T_m of the C180Y mutant is close to the physiological temperature of the human body, it is less likely that its functional activity could be retained in the human brain. Other STXBP1 mutants (p.V84D, p.G544D, and p.M443R) tend to form aggregates, and thus sufficient protein for biophysical analyses could not be obtained.

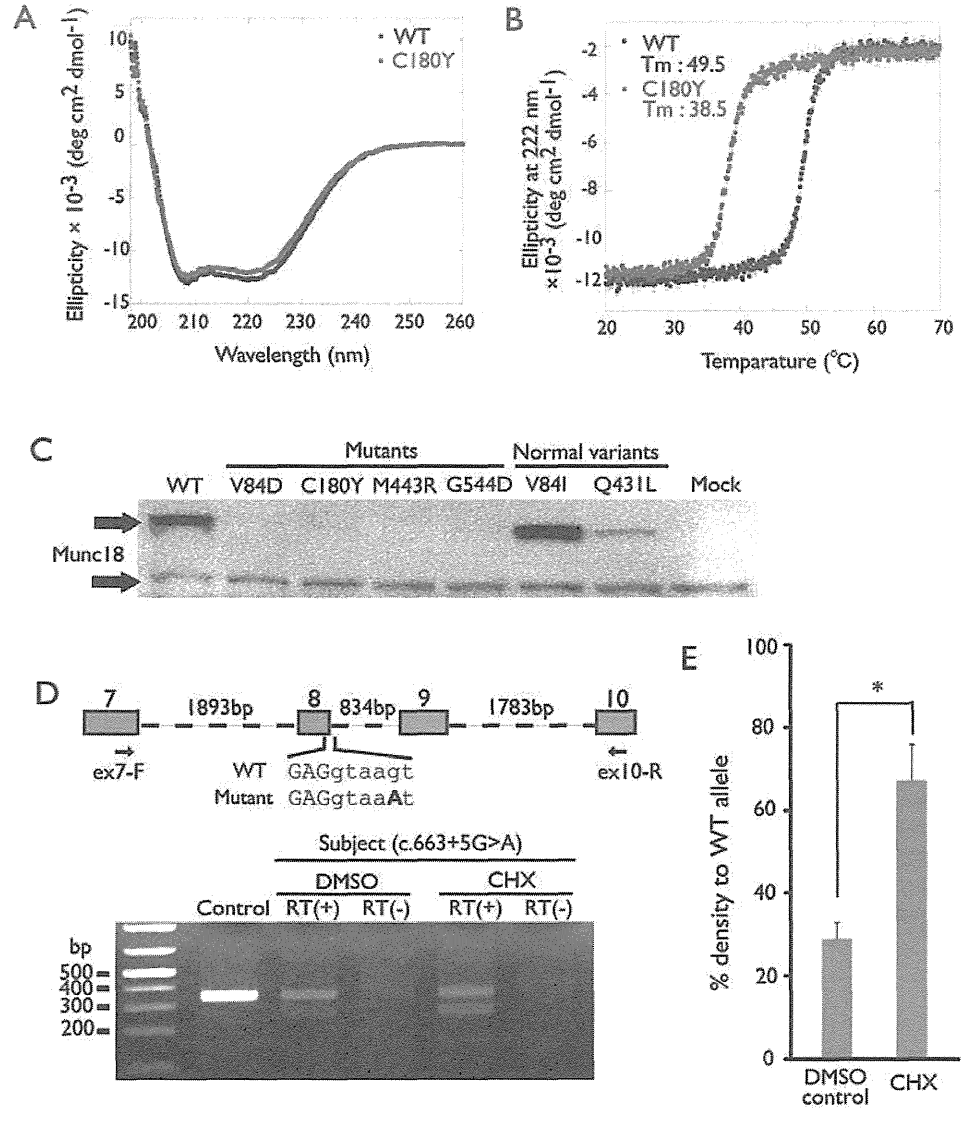

Figure 3. Characterization of mutant STXBP1 proteins and mRNAs with aberrant splicing

(A) Circular dicroism spectra of the WT and C180Y-mutated STXBP1. The C180Y mutation is found to induce a subtle decrease in the helical contents of the STXBP1 structure by comparing the peaks of both proteins at 222 nm, where a large negative ellipticity

value indicates a high helical content of the protein. (B) Circular dicroic melting curves of the STXBP1 WT and C180Y proteins. Values of ellipticity at 222 nm are measured to monitor the thermal unfolding of the proteins. The C180Y mutant became unfolded at a lower temperature compared to the WT. Each dot represents the average of three repeated experiments, with standard deviations depicted as error bars. (C) Immunoblot analysis of mutant STXBP1 proteins using a monoclonal anti-Munc18 antibody. Upper and lower bands represent EGFP-STXBP1 and endogenous STXBP1 proteins, respectively. Expression of four mutant STXBP1 proteins was not detected, while the WT and two normal variants could be detected. (D) (Top) Schematic representation of the genomic structure from exons 7 to 10 of *STXBP1*. Exons, introns, and primers are shown by boxes, dashed lines, and arrows, respectively. Sequences of exons and introns are presented in uppercase and lower-case, respectively. The mutation in intron 8 is highlighted in bold. (Bottom) Reverse transcriptase-PCR analysis of patient #11 with a c.663+5G>A mutation and a normal control. Two PCR products were detected from the patient's cDNA: the upper one is the WT transcript and the lower one is the mutant. Only a single WT amplicon was detected in the control. The mutant amplicon was significantly increased by 30 μM cycloheximide (CHX) treatment compared to dimethyl sulfoxide (DMSO) treatment as a vehicle control. RT (+): with reverse transcriptase, RT (−): without reverse transcriptase as a negative control. (E) Quantitative analysis of the NMD inhibition by CHX based on the data shown in (D). $*P = 0.0023$ by unpaired Student's *t*-test, two tailed. Averages of three repeated experiments are shown with error bars (s.d). Adapted from Refs. [9] and [19]

Degradation of Mutant STXBP1 Proteins

Transient expression of mutant STXBP1 proteins in Neuroblastoma 2A (N2A) cells showed further evidence of *STXBP1* haploinsufficiency. The WT EGFP-STXBP1 was expressed in the cytosolic compartment, but not in the nucleus or plasma membrane, similar to endogenous expression.[9,23] However, in approximately 20% of cells expressing mutant EGFP-STXBP1 (p.V84D, p.C180Y, p.M443R, and p.G544D), intense clusters of fluorescence signals were observed, likely representing protein aggregation.[9] The other 80% of cells showed a diffuse cytosolic protein distribution similar to that expressing the WT, but the signal intensity was much weaker, implying possible protein degradation. Protein degradation of mutant STXBP1 proteins was also confirmed by immunoblotting using an anti-Munc18 antibody[19] (Figure 3C). These experiments suggested that mutant STXBP1 proteins would be aggregated or degraded in neurons, both leading to loss of STXBP1 function.

Degradation of *STXBP1* mRNA with Abnormal Splicing

The splicing, frameshift, and nonsense mutations would produce a premature stop codon; therefore, these mutant mRNAs are likely to be degraded by NMD.[24,25] In fact, NMD associated with abnormal splicing was demonstrated in lymphoblastoid cells derived from a patient harboring a c.663+5G>A mutation. Polymerase chain reaction (PCR) primers designed to amplify exons 7 to 10 amplified a single band (338 bp), corresponding to the WT *STXBP1* allele, using a cDNA template from a control lymphoblastoid cell lines (LCL; Figure 3D). By contrast, a smaller band was detected from the patient's cDNA, in which exon 8 of *STXBP1* was skipped (Figure 3D), resulting in the insertion of nine new amino acids followed by a premature stop codon at position 203. Moreover, the intensity ratio of the mutant compared to the normal band was increased by up to 67 % after treatment with 30 μM cycloheximide, which inhibits NMD, compared to a ratio of 29 % in the untreated condition (Figure 3D, E). These facts suggest that the mutant mRNA possessing a premature stop codon suffered from degradation by NMD in neurons, resulting in haploinsufficiency.

Considering the degradation of STXBP1 proteins with missense mutations, NMD of mRNAs with premature stop codons and the effects of deletion of STXBP1, we conclude that haploinsufficiency of *STXBP1* causes OS.

HOW WOULD HAPLOINSUFFICIENCY OF *STXBP1* LEAD TO OS?

Impairment of Synaptic Vesicle Release

STXBP1 (*MUNC18-1*) is a member of the evolutionarily conserved Sec1/Munc-18 gene family that acts at specific steps of intracellular membrane transport.[26,27] In mammalian exocytosis, the vesicular SNARE protein, VAMP2 (also known as *synaptobrevin2*), and the target

Jasper's Basic Mechanisms of the Epilepsies

membrane SNARE proteins, Syntaxin-1 and SNAP25, constitute the core fusion machinery that bring two membranes into close apposition to fuse.[22,28] An *Stxbp1* null mutation led to complete loss of neurotransmitter secretion from synaptic vesicles throughout development in mice, though seizures have never been described.[16] Thus, *STXBP1* very likely plays a central role in synaptic vesicle release in coordination with SNARE proteins. The association of mutations of *STXBP1* with OS implies that perturbation of synaptic vesicle release forms part of the genetic basis of epilepsy. To date, the majority of genes associated with epilepsy syndromes are ion channel genes.[29] Synapsin I is a synaptic vesicle protein thought to regulate the kinetics of neurotransmitter release during priming of synaptic vesicles, and a mutation has been identified in a family with X-linked epilepsy and learning difficulties.[30] *STXBP1* is the second synaptic vesicle gene shown to be involved in epilepsy, and this finding will encourage further research into regulation of synaptic vesicle release and its involvement in seizures and related disorders.

Possible Interneuropathy

In *Stxbp1* heterozygous knockout mice, no seizures have been reported, and whole-cell recordings of autaptic glutamatergic or GABAergic (GABA: gamma-aminobutyric acid) neurons showed excitatory and inhibitory postsynaptic currents similar to those of WT littermate neurons upon single depolarizations.[31] However, with repeated stimulation, $Stxbp1^{+/-}$ neurons showed impaired synaptic function due to the reduced size and replenishment rate of readily releasable vesicles,[31] suggesting that heterozygous deletion of *Stxbp1* indeed affected synaptic function in mice. Interestingly, the reduction of readily releasable vesicles was more evident in GABAergic neurons than in glutamatergic neurons.[31] It has been reported that *Arx* is expressed in GABAergic interneurons, and that *Arx* controls their genesis, migration, and differentiation, as *Arx*-knockout mice showed a deficit of GABAergic interneurons.[32] Moreover, neuropathological examination of three patients with X-linked lissencephaly with absent corpus callosum and ambiguous genitalia, caused by *ARX* mutations, has suggested a loss of interneurons.[33] If haploinsufficiency of *STXBP1* affected GABAergic interneurons more severely than glutamatergic neurons in humans as in mice, a defect in the GABAergic system could be postulated as a common pathophysiology among OS patients with *ARX* or *STXBP1* mutations. Ohtahara syndrome might be designated as a continuum of "interneuronopathies".[34,35]

Cell Death of the Brainstem

As brain malformations are often associated with individuals with OS,[2,3] it could be speculated that *STXBP1* mutations would lead to abnormal brain structures directly related to the seizure phenotype of OS. However, we did not observe structural brain anomalies in any of the 14 OS patients with *STXBP1* defects. This is consistent with the findings that mice deleted for *Stxbp1* have normal brain architecture. *Stxbp1* null mice, however, showed extensive cell death of mature neurons in lower brain areas, such as the brainstem; the lower brainstem was almost completely lost by embryonic day 18.[16] This is consistent with the suggestion that tonic seizures in OS might originate from subcortical structures, including the brainstem. Thus, in addition to the impaired synaptic vesicle release, it is possible that *STXBP1* haploinsufficiency leads to OS through microscopically impaired neuronal cell death in lower brain areas.

FUTURE CHALLENGES

Expansion of the Clinical Spectrum of *STXBP1* Mutations

Although OS is the core phenotype of *STXBP1* defects in our Japanese cohort (one third of OS cases harbored *STXBP1* mutations), Hamdan et al. recently reported that two *de novo* *STXBP1* mutations, c.1162C>T (p.R388X) and c.169+1G>A, were identified in 2 out of 95 individuals with MR and nonsyndromic epilepsy.[36] According to their report, the two patients

never showed the tonic seizures or infantile spasms associated with OS and WS, respectively. The onset of first seizures was at 6 weeks and 2 years of age, respectively. In addition, characteristic EEG patterns, such as suppression-burst or hypsarrhythmia, were never observed in these patients. Thus, the finding by Hamdan et al. indicated that *STXBP1* defects could cause a wide spectrum of clinical epileptic disorders in association with severe MR. Given that defects in synaptic dysfunction have also been implicated in many common neurodevelopmental disorders, such as MR, autism, and schizophrenia,[37,38] the possible involvement of *STXBP1* mutations in such common neurodevelopmental disorders is of interest. Elucidation of the molecular basis of synaptic vesicle processing disturbed by *STXBP1* mutations will allow us to understand not only the pathophysiology of infantile epilepsy, but also many neuropsychiatric conditions that present beyond childhood. The contribution of *STXBP1* mutations to EME also should be clarified, because myoclonic seizures, the characteristic feature of EME, are occasionally observed in 3/14 patients with *STXBP1* mutations.

Animal Model

An animal model is necessary to elucidate the pathophysiology of epilepsy caused by *STXBP1* mutations, including age-dependency of seizure type and EEG pattern, and to test potential therapies directed specifically at OS and subsequent WS. The effect of gene dosage alterations of *STXBP1/Stxbp1* might vary between humans and mice: humans might be more susceptible than mice; thus, loss of function of one allele could cause seizures in humans but not in mice. Although it would be challenging to manipulate the gene dosage of *Stxbp1* - for example, in combination with a hypomorphic allele and a null allele - to the level at which mutant mice show a seizure phenotype, the establishment of an animal model will greatly benefit our understanding of the mechanisms of seizures in relation to impaired synaptic function.

References

1. Ohtahara S, Ishida T, Oka E, Yamatogi Y, Inoue H, Karita S, Ohtsuka Y. [On the specific age dependent epileptic syndrome: the early-infantile epileptic encephalopathy with suppression-burst.]. No to Hattatsu 1976;8:270–279.
2. Djukic A, Lado FA, Shinnar S, Moshe SL. Are early myoclonic encephalopathy (EME) and the Ohtahara syndrome (EIEE) independent of each other? Epilepsy Res 2006;70(Suppl 1):S68–76. [PubMed: 16829044]
3. Ohtahara S, Yamatogi Y. Ohtahara syndrome: with special reference to its developmental aspects for differentiating from early myoclonic encephalopathy. Epilepsy Res 2006;70(Suppl 1):S58–67. [PubMed: 16829045]
4. Yamatogi Y, Ohtahara S. Early-infantile epileptic encephalopathy with suppression-bursts, Ohtahara syndrome; its overview referring to our 16 cases. Brain Dev 2002;24:13–23. [PubMed: 11751020]
5. Kato M, Saitoh S, Kamei A, Shiraishi H, Ueda Y, Akasaka M, Tohyama J, Akasaka N, Hayasaka K. A Longer Polyalanine Expansion Mutation in the ARX Gene Causes Early Infantile Epileptic Encephalopathy with Suppression-Burst Pattern (Ohtahara Syndrome). Am J Hum Genet 2007;81:361–366. [PubMed: 17668384]
6. Fullston T, Brueton L, Willis T, Philip S, MacPherson L, Finnis M, Gecz J, Morton J. Ohtahara syndrome in a family with an ARX protein truncation mutation (c.81C>G/p.Y27X). Eur J Hum Genet 2010;18:157–162. [PubMed: 19738637]
7. Absoud M, Parr JR, Halliday D, Pretorius P, Zaiwalla Z, Jayawant S. A novel ARX phenotype: rapid neurodegeneration with Ohtahara syndrome and a dyskinetic movement disorder. Dev Med Child Neurol 2009;3:305–307.
8. Kato M, Koyama N, Ohta M, Miura K, Hayasaka K. Frameshift mutations of the ARX gene in familial Ohtahara syndrome. Epilepsia 2010;51:1679–1684. [PubMed: 20384723]
9. Saitsu H, Kato M, Mizuguchi T, Hamada K, Osaka H, Tohyama J, Uruno K, Kumada S, Nishiyama K, Nishimura A, Okada I, Yoshimura Y, Hirai S, Kumada T, Hayasaka K, Fukuda A, Ogata K,